Fig. 1. Clinical course of the SOS. FK506 = Tacrolimus; mPSL = methylprednisolone; rTM = recombinant human soluble thrombomodulin; AT-III = antithrombin III; FFP = fresh frozen plasma; PL = platelet transfusion; CHDF = continuous hemodiafiltration.

developed, but this resolved with topical steroid treatment. Although his neutrophil count reached $0.5 \times 10^9/l$ on day 27 and he subsequently achieved complete donor chimerism, there was persistent thrombocytopenia that was refractory to platelet transfusion.

Ultrasonography on day 28 showed ascites, and progressive hepatomegaly and renal dysfunction developed simultaneously. Despite administration of fresh frozen plasma and AT-III together with danaparoid, recombinant human soluble thrombomodulin and methylprednisolone, his hyperbilirubinemia worsened. Continuous hemodialysis was initiated for the hepatorenal syndrome from day 52, but the patient died of multiple organ failure on day 69 (fig. 1). At autopsy, the liver showed hepatocellular necro-

sis in addition to thickening of the subintimal zone, mainly in zone 3 of the acini, occlusion and congestion of the central hepatic venules, and a large amount of bile thrombus, findings consistent with the histopathology of SOS.

Flow reversal in segmental branches of the portal vein or visualization of the paraumbilical vein on ultrasonography have been reported to be associated with SOS [6–8]. After clinical diagnosis of SOS we performed ultrasonography weekly. While we could neither detect hepatofugal portal flow nor visualize the paraumbilical vein, we did find hepatomegaly relative to the baseline size of the liver (fig. 1). We also performed per rectal portal scintigraphy on day 62. Per rectal portal scintigraphy is a noninvasive method for evaluation of portosystemic shunting using
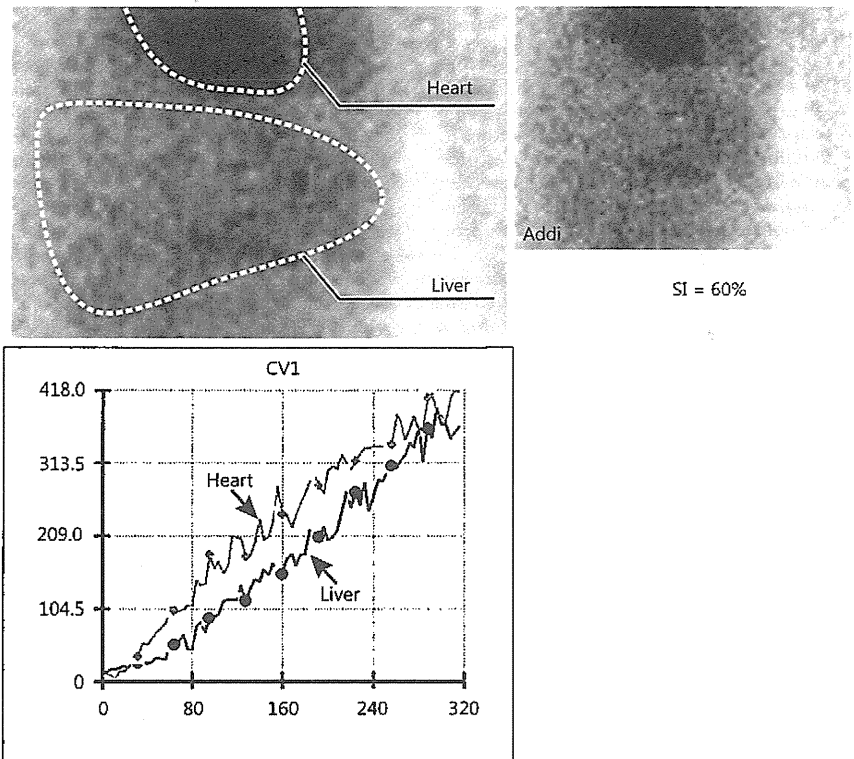
Okamura/Hayashi/Nakamae/Shiomi/
Nishimoto/Koh/Nakane/Hino

Fig. 2. Per rectal portal scintigram in this case. The radioactivity curves of the liver and the heart are obtained from the images based on the concentration of ^{99m}Tc entering the liver and the heart.

the portal shunt index (SI), calculated from radioactivity curves of the liver and the heart. Radioactive tracer absorbed from the rectum passes through the inferior mesenteric vein into the portal vein, the liver and then the right heart. Ten millicuries (2 ml) of [^{99m}Tc] pertechnetate, followed by 15 ml of air, are given through a polyethylene tube (Nelaton catheter, F 18) inserted deep into the rectum to avoid absorption into the systemic circulation via the inferior rectal veins of the lower rectum. The radioactivity curves of the liver and the heart are then obtained from the images that depict these organs, using a large-field scintillation detector (Technicare-410S, Technicare, Solon, Ohio, USA) positioned over the patient's abdomen. In patients with chronic liver disease, the SI correlates well with portal pressure measured by percutaneous transhepatic portography or an intraoperative method. It was reported that SI values of 10% or higher are abnormal [9]. In this case, the examination was performed safely and the shunt index of 60% indicated severe portal hypertension (fig. 2).

A hepatic venous pressure gradient above 10 mmHg is highly specific for histologically confirmed SOS. This gradient value provides 91% specificity and an 86% positive predictive value [5]. In our case of severe SOS we could not detect the condition on ultrasonography, despite the use of pulsed Doppler ultrasound. Per rectal portal scintigraphy was performed in the late phase of SOS. Although SOS should be diagnosed at an early stage so that treatment can be started, the SI may not reveal mild abnormalities in the portal circulation in the absence of extrahepatic shunts. It was also reported that the liver transit time (LTT) is useful in the detection of the early phase of portal hypertension, without portosystemic shunts. The LTT is the time interval between the entrance of radioactive tracer into the liver and its subsequent entrances into the right heart, after absorption from the upper rectum and passage through the mesenteric and portal veins [10]. The significance of the LTT should be assessed in a clinical trial of its utility in detecting the early phase of SOS.

The present case suggests that per rectal portal scintigraphy is potentially a safe, sensitive method of detecting SOS and offers a new diagnostic strategy that complements clinical criteria. Further prospective studies will be needed to clarify the utility and prognostic value of per rectal portal scintigraphy in the diagnosis of SOS.

Portal Scintigraphy for Detection of SOS

85

References

1 Coppell JA, Richardson PG, Soiffer R, Martin PL, Kernan NA, Chen A, Guinan E, Vogelsang G, Krishnan A, Giralt S, Revta C, Carreau NA, Iacobelli M, Carreras E, Ruutu T, Barbui T, Antin JH, Niederwieser D: Hepatic veno-occlusive disease following stem cell transplantation: incidence, clinical course, and outcome. Biol Blood Marrow Transplant 2010;16:157–168.

2 Ho VT, Revta C, Richardson PG: Hepatic veno-occlusive disease after hematopoietic stem cell transplantation: update on defibrotide and other current investigational therapies. Bone Marrow Transplant 2008;41:229–237.

3 Maradei SC, Maiolino A, de Azevedo AM, Colares M, Bouzas LF, Nucci M: Serum ferritin as risk factor for sinusoidal obstruction syndrome of the liver in patients undergoing hematopoietic stem cell transplantation. Blood 2009;114:1270–1275.

4 Carreras E, Grañena A, Navasa M, Bruguera M, Marco V, Sierra J, Tassies MD, García-Pagán JC, Martí JM, Bosch J: On the reliability of clinical criteria for the diagnosis of hepatic veno-occlusive disease. Ann Hematol 1993;66:77–80.

5 Shulman HM, Gooley T, Dudley MD, Kofler T, Feldman R, Dwyer D, McDonald GB: Utility of transvenous liver biopsies and wedged hepatic venous pressure measurements in sixty marrow transplant recipients. Transplantation 1995;59:1015–1022.

6 Lassau N, Leclère J, Auperin A, Bourhis JH, Hartmann O, Valteau-Couanet D, Benhamou E, Bosq J, Ibrahim A, Girinski T, Pico JL, Roche A: Hepatic veno-occlusive disease after myeloablative treatment and bone marrow transplantation: value of gray-scale and Doppler US in 100 patients. Radiology 1997; 204:545–552.

7 Hashiguchi M, Okamura T, Yoshimoto K, Ono N, Imamura R, Yakushiji K, Ogata H, Seki R, Otsubo K, Oku E, Kuroiwa M, Higuchi M, Kato K, Taniguchi S, Gondo H, Shibuya T, Nagafuji K, Harada M, Sata M: Demonstration of reversed flow in segmental branches of the portal vein with hand-held color Doppler ultrasonography after hematopoietic stem cell transplantation. Bone Marrow Transplant 2005;36:1071–1075.

8 McCarville MB, Hoffer FA, Howard SC, Goloubeva O, Kauffman WM: Hepatic veno-occlusive disease in children undergoing bone-marrow transplantation: usefulness of sonographic findings. Pediatr Radiol 2001;31: 102–105.

9 Shiomi S, Kuroki T, Kurai O, Kobayashi K, Ikeoka N, Monna T, Ochi H: Portal circulation by technetium-99m pertechnetate perrectal portal scintigraphy. J Nucl Med 1988; 29:460–465.

10 Dragoteanu M, Balea IA, Dina LA, Piglesan CD, Grigorescu I, Tamas S, Cotul SO: Staging of portal hypertension and portosystemic shunts using dynamic nuclear medicine investigations. World J Gastroenterol 2008;14: 3841–3848.

Review

Role of endothelial-mesenchymal transition in idiopathic portal hypertension

Yasunori Sato and Yasuni Nakanuma

Department of Human Pathology, Kanazawa University Graduate School of Medicine, Kanazawa, Japan

Summary. Idiopathic portal hypertension (IPH) is a condition of non-cirrhotic portal hypertension without a known cause of liver disease. Obliterative portal venopathy is regarded as the primary lesion, which is responsible for the pre-sinusoidal block of hepatic blood flow leading to the development of IPH. The disease pathogenesis of IPH seems to be heterogeneous, and the pathogenic mechanisms of obliterative portal venopathy have not been fully understood. Owing to the limited understanding of the disease pathogenesis, the treatment of IPH is still largely supportive. Recently, endothelial dysfunction has been documented during the development of portal hypertension, and its contribution to IPH is being analyzed. Endothelial-mesenchymal transition (EndMT) is a phenomenon whereby vascular endothelial cells acquire myofibroblastic features characterized by an ability to express mesenchymal cell products that are related to tissue fibrogenesis. In addition to cardiovascular development, there is increasing evidence showing that EndMT is likely to be involved in a variety of fibrotic diseases, such as cardiac, pulmonary, and renal fibrosis. This article reviews the recent progress in studies of the pathogenic mechanisms of IPH in terms of endothelial dysfunction of portal veins. In particular, the role of EndMT in obliterative portal venopathy of IPH is highlighted and discussed.

Key words: Idiopathic portal hypertension, Endothelial-mesenchymal transition, Obliterative portal venopathy, Hepatoportal sclerosis, Fibroelastosis

Introduction

Idiopathic portal hypertension (IPH) is defined as a condition of non-cirrhotic portal hypertension in the absence of a known cause of liver disease and with a patent extrahepatic portal vein (Nakanuma et al., 2001; Schouten et al., 2011). It is also referred to as hepatoportal sclerosis and non-cirrhotic portal fibrosis, although there have been several differences in the application of these terms. Portal hypertension in patients with IPH arises because of pre-sinusoidal obstruction of hepatic blood flow. Obliterative venopathy with luminal narrowing or obliteration of small portal veins accompanied by dense deposits of elastic fibers is one of the most characteristic findings in the liver histology of IPH, which is responsible for the pre-sinusoidal block of hepatic blood flow (Nakanuma et al., 1996; Chawla and Dhiman, 2008; Cazals-Hatem et al., 2011).

IPH is considered a disorder with a relatively benign disease course, but progression to liver failure, hepatic encephalopathy, and hepatopulmonary syndrome has been encountered (Sawada et al., 2007; Eapen et al., 2011). In a proportion of cases, indications for liver transplantation are considered (Bernard et al., 1995; Krasinskas et al., 2005; Isabel Fiel et al., 2007). Many etiological factors related to the development of IPH have been proposed, including immunological disorders, chronic infections, exposure to medication or toxins, genetic disorders, and thrombophilia (Schouten et al.,

2011). The disease pathogenesis of IPH seems to be heterogeneous, and the pathogenic mechanisms of obliterative portal venopathy have not been fully understood. Owing to the limited understanding of the disease pathogenesis, treatment of IPH remains largely supportive and is directed toward treating complications of portal hypertension (mainly variceal bleeding and splenomegaly) (de Franchis, 2010).

Recently, endothelial dysfunction has been documented during the development of portal hypertension, as well as liver cirrhosis, and its contribution to IPH is being analyzed (Iwakiri, 2012). This article reviews the recent progress in studies of the pathogenic mechanisms of IPH in terms of endothelial dysfunction of portal veins, particularly focusing on the role of endothelial-mesenchymal transition (EndMT) in obliterative portal venopathy. First, the pathological features of IPH are briefly described to obtain a better understanding of the disease pathogenesis.

Pathological features of IPH

Gross pathology

Macroscopic features in IPH may vary according to the extent of disease progression, and they have been examined mainly in livers obtained from pathological autopsies and liver transplantation. The majority of these livers show atrophy and dysmorphy, and old occluding or mural thrombi are frequently seen in the large portal vein branches (Nakanuma et al., 2001; Sawada et al., 2007). In some patients, gross appearance is normal, and nodular appearance and dilatation of the portal vein trunk can also be encountered (Nakanuma et al., 2001).

Histopathology

The pathological features of IPH livers are not pathognomonic. Frequently observed histological features include obliterative portal venopathy of small portal veins, periportal/perisinusoidal fibrosis, and dilated portal veins herniating into the surrounding parenchyma (Nakanuma et al., 2001; Okudaira et al., 2002; Tsuneyama et al., 2003). Obliterative portal venopathy is generally regarded as the primary lesion accounting for the development of IPH (Cazals-Hatem et al., 2011).

Portal tracts often show collagen deposition, and dense deposition of elastic fibers accompanied by obliterated small portal vein is also a characteristic finding (Fig. 1). They are irregularly distributed in an individual liver. Portal tracts are variably enlarged, and occasionally show thin fibrous septa growing into the hepatic parenchyma. Portal inflammation is typically negligible. In some patients, hepatic fibrosis corresponds to incomplete septal cirrhosis (Roskams et al., 2003; Hübscher, 2011). The fibrogenic process may be mediated partially by activated hepatic stellate cells (Tsuneyama et al., 2002).

Hilar and intrahepatic large and medium-sized portal veins are open or even dilated in established IPH livers. Phlebosclerosis is a common finding, and the major portal vein branches show fibroelastosis and intimal thickening to various degrees (Fig. 2). In the advanced disease stage, they are occasionally occluded by old thrombi with recanalization.

Atrophy of hepatic parenchyma, which is accentuated in the subcapsular region, is often observed during disease progression. Such cases are preferentially observed in perivenular areas and between hyperplastic hepatic nodules. Hepatocytes are more or less atrophic or small, and apoptosis of hepatocytes is occasionally seen (Tsuneyama et al., 2002). In some cases, the liver histology is almost normal, except for portal venous dilatation or obliteration. Hyperplastic lesions such as nodular regenerative hyperplasia and partial nodular
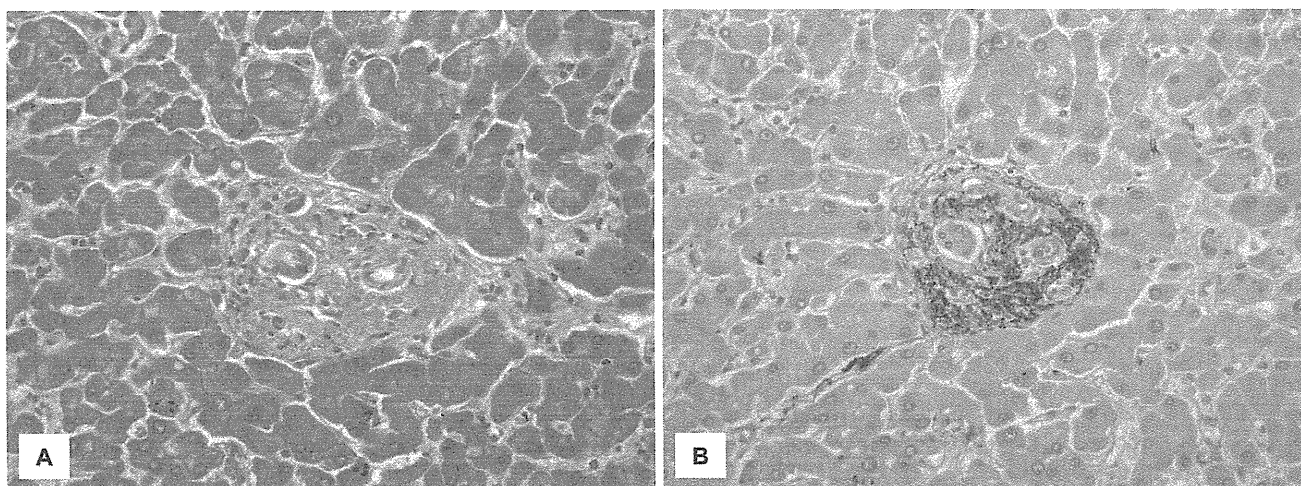

Fig. 1. Fibrotic portal tract of IPH with obliterated small portal vein. **A,** Azan-Mallory staining; **B,** Elastica-van Gieson staining.

transformation are encountered in a proportion of cases, which may result from disturbed intrahepatic circulation (Wanless, 1990; Nakanuma et al., 1996).

EndMT

General aspects

During the development and progression of pathological fibrosis, myofibroblasts play an important role in the production of extracellular matrix molecules. Myofibroblasts are derived from at least three sources:

Fig. 2. Hilar portal vein of IPH with fibroelastosis and an organized thrombus. Elastica-van Gieson staining.

resident tissue fibroblasts, transition of epithelial cells into mesenchymal cells (epithelial-mesenchymal transition, EMT), and bone marrow-derived circulating fibrocytes (Wynn, 2008).

Recently, EndMT has emerged as another possible source of tissue myofibroblasts (Piera-Velazquez et al., 2011; Kovacic et al., 2012). EndMT is a complex biological process that is recognized as cellular transdifferentiation characterized by the down-regulation of vascular endothelial markers such as CD31 and von Willebrand factor, and the emergence of myofibroblastic markers such as S100A4/fibroblast-specific protein-1 and α-smooth muscle actin (α-SMA). Endothelial cells that undergo EndMT acquire an ability to express mesenchymal cell products such as type I collagen, thereby contributing to the fibrotic process.

Associated conditions and diseases

The essential role of EndMT in cardiovascular development has been thoroughly studied (Kovacic et al., 2012). Recently, increasing evidence has been accumulated showing that EndMT is likely to be involved in a variety of fibrotic diseases. The involvement of EndMT has been shown in cardiac, pulmonary, and renal fibrosis (Zeisberg et al., 2007). In corneal injury, acute inflammatory response following the injury is regarded as important in the induction of EndMT (Lee et al., 2012). The role of inflammation-induced EndMT has also been investigated in intestinal fibrosis, indicating its role in chronic inflammatory diseases such as inflammatory bowel disease (Rieder et al., 2011). Carcinoma-associated interstitial fibrosis has been shown to be mediated by EndMT (Zeisberg et al., 2007).
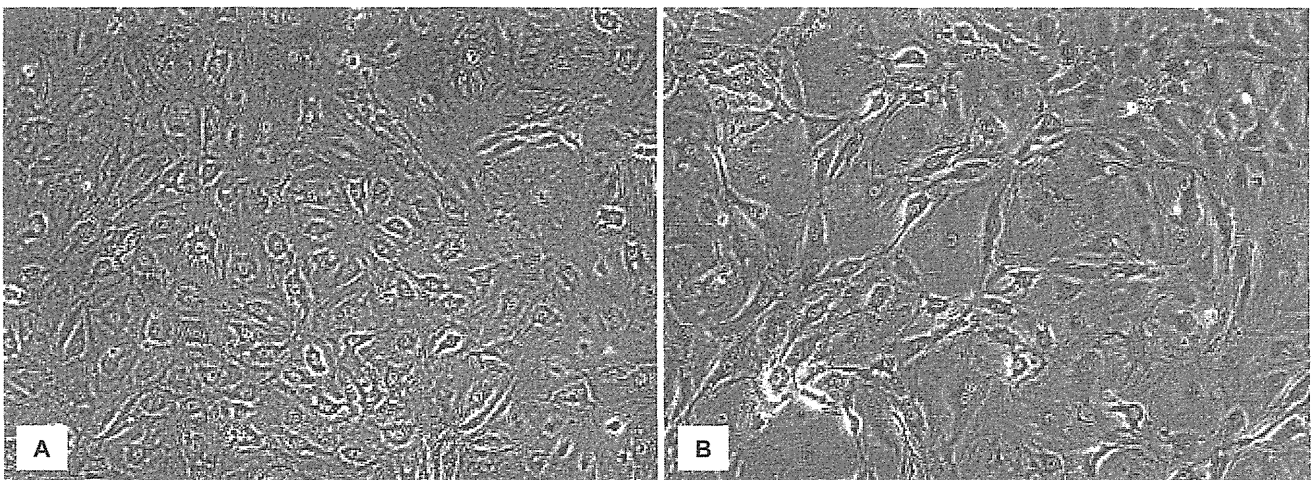

Fig. 3. Morphological alteration of human dermal microvascular endothelial cells (HMVEC) by TGF-ß1. HMVEC grow in the form of an epithelioid, sheet-like appearance **(A)**, and treatment with TGF-ß1 changes the cellular morphology from an epithelioid to a spindle-shaped appearance **(B)**. Phase-contrast microscopy.

Systemic sclerosis (SSc) is another example in which the process of EndMT may be involved in the disease pathogenesis (Karasek, 2007). Of relevance, SSc bears many of the hallmarks of conditions involving EndMT, including mesenchymal cell proliferation and TGF-ß signaling. Although a chronic inflammatory condition affecting the vasculature is considered to be related to the occurrence of EndMT (Chaudhuri et al., 2007), an established lesion of dense cutaneous fibrosis in SSc usually lacks significant inflammatory cell infiltrates, which is similar to the histological lesion of hepatoportal sclerosis of IPH.

In the liver, the fibrogenic process is mediated by myofibroblasts in most types of chronic liver disease, which originate from hepatic stellate cells. Fibrogenic liver injury is often accompanied by portal and/or parenchymal inflammation. Because α-SMA-positive activated hepatic stellate cells are focally found in the perisinusoidal area of IPH livers, parenchymal fibrosis may be explained by the contribution of myofibroblasts (Tsuneyama et al., 2002). However, α-SMA-positive myofibroblast-like cells are rarely seen in the peripheral portal tracts of IPH, suggesting that other matrix-producing cells may exist in the portal tracts.

In addition to residual portal fibroblasts, EndMT may contribute to portal fibrosis of IPH (Kitao et al., 2009), although the role of EndMT in hepatic fibrogenesis has not been fully studied. The contribution of bone marrow-derived fibrocytes, as well as the process of EMT of hepatocytes and biliary epithelial cells, is still under debate (Higashiyama et al., 2009; Popov and Schuppan, 2010; Wells, 2010; Scholten et al., 2011).

Molecular mechanisms

Transforming growth factor-ß (TGF-ß) plays a crucial role in tissue fibrosis and is implicated in the pathogenesis of numerous disorders. Similar to EMT, TGF-ß acts as a potent inducer of EndMT both *in vitro* and *in vivo*. In fact, human dermal microvascular endothelial cells (HMVEC) undergo morphological alteration from an epithelioid, sheet-like appearance into a spindle-shaped, myofibroblastic-like appearance following TGF-ß1 treatment *in vitro* (Fig. 3). The spindle-shaped HMVEC following TGF-ß1 treatment has been shown to exhibit reduced expression of a vascular endothelial cell marker, CD34, and increased expression of S100A4, α-SMA, COL1A1, and pSmad2 (Kitao et al., 2009).

During cardiovascular development, TGF-ß2, TGF-ß3, and bone morphogenic proteins 2 and 4 (BMP-2 and -4) are required for initiation and completion of EndMT (Armstrong and Bischoff, 2004). Crucial roles of signaling pathways, including wnt/ß-catenin and Notch, have been suggested in the process (Gitler et al., 2003; Luna-Zurita et al., 2010). Endocardial EndMT is also dependent on receptor tyrosine kinase signaling via the phospho-inositide-3 kinase-phosphoinositide-dependent protein kinase 1-Akt/protein kinase B cascade, which is upstream of Snail (Kovacic et al., 2012). Recently, differential expression or microRNA has been analyzed during cardiac EndMT (Ghosh et al., 2012).

TGF-ß binds to TGF-ß receptor type II (TßR-II), and recruits the TGF-ß receptor type I (TßR-I). TßR-I subsequently phosphorylates Smad2 and Smad3, and they translocate from the cytoplasm to the nucleus, where they regulate transcription of target genes. BMP-7 is a member of the TGF-ß superfamily, and a promising TGF-ß antagonist by counteracting Smad2/3 phosphorylation (Kinoshita et al., 2007). Indeed, it has been shown that BMP-7 inhibits the TGF-ß1-induced EndMT in HMVEC *in vitro*, and it was also shown to abrogate EndMT induced by TGF-ß1 in a mouse model
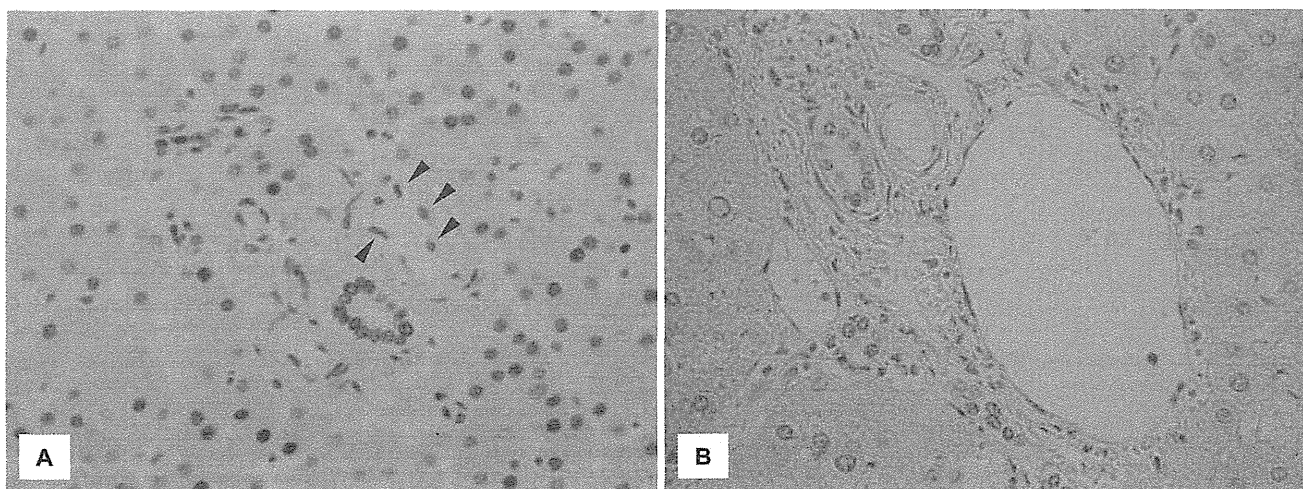

Fig. 4. Increased immunohistochemical expression of pSmad2 in IPH liver. Arrowheads indicate pSmad2-positive endothelial cells of peripheral portal tract of IPH. **A.** IPH. **B.** Normal liver.

of cardiac fibrosis *in vivo* (Zeisberg et al., 2007). In addition, the blockade of EndMT by a Smad3 inhibitor was found to delay the development of diabetic nephropathy in a mouse model (Li et al., 2010).

EndMT also occurs independently of Smad2/3 activation. The non-Smad pathway of TGF-ß signaling involves the participation of several kinases, including the c-Abl protein kinases, protein kinase Cδ, and glycogen synthase kinase 3ß, and the kinase inhibitor molecules have been suggested to be effective therapeutic agents for SSc (Li et al., 2011). Inflammatory cytokines, such as interleukin-1ß, also play a role in the initiation of EndMT. Importantly, EndMT may be a reversible process (Arciniegas et al., 2007), and therefore represents a novel therapeutic target for fibrotic disorders.

EndMT in IPH

Overlap of IPH and SSc

IPH has frequently been reported in association with immunological disorders, including SSc, systemic lupus erythematosus, rheumatoid arthritis, mixed connective tissue disease, and celiac disease (Tsuneyama et al., 2002; Schouten et al., 2011). Various theories have been proposed to explain this.

SSc is a disease that causes excessive collagen production and deposition, vascular damage, and inflammation in multiple organs including skin, lung, and the gastrointestinal tract. Patients with the disease show increased deposition of collagen types I and III in various organs, with type I being the most abundant (Charles et al., 2006). Given the etiological fact that SSc is a clinical complication of IPH, it is possible that similar pathogenic mechanisms of collagen deposition exist between IPH and SSc (Nakanuma et al., 2009). Because EndMT is believed to be involved in excessive collagen deposition in patients with SSc, it may also be related to the portal fibrosis of IPH. In the following sections, the role of EndMT in obliterative portal venopathy of IPH is discussed on the basis of the results of our study (Kitao et al., 2009).

EndMT in IPH liver

Many IPH livers show diffuse and strong nuclear expression of pSmad2 throughout the liver, including portal vein endothelium, hepatocytes, and biliary epithelial cells (Fig. 4A). In contrast, positive immunohistochemical expression of pSmad2 is rarely seen in sections of normal liver (Fig. 4B). Since both TßR-I and TßR-II are diffusely expressed in the liver, including portal vein endothelium of IPH as well as normal liver, the increased expression of pSmad2 in the IPH livers may reflect the activation of the signaling pathways, including TGF-ß, leading to the occurrence of EndMT in the endothelium.

Diffuse and strong immunoexpression of pSmad2 in

hepatocytes, as well as portal vein endothelium in IPH livers, also indicates that hepatic parenchymal atrophy frequently seen in IPH patients at an advanced disease stage may be associated with the growth inhibitory effects of TGF-ß on hepatocytes, as well as the circulatory disturbance of the liver, because TGF-ß has an effect of growth inhibition or induction of apoptosis on hepatocytes (Nguyen et al., 2007).

In the peripheral portal tracts of IPH liver, reduction of the immunohistochemical expression of CD34 in the endothelial cells of the peripheral portal vein is frequently observed compared with that of the escorting hepatic artery in the same portal tract. The reduction of CD34 expression is seen in peripheral portal veins of IPH regardless of the presence or absence of luminal narrowing. The reduction of CD34 expression in the portal vein endothelium significantly correlates with the induction of pSmad2 expression, suggesting a causal relationship between them *in vivo*.

Double immunofluorescence staining of CD34 and S100A4 protein shows that portal vein endothelium of IPH occasionally co-expresses CD34 and S100A4 (Fig. 5, arrowhead), suggesting the occurrence of EndMT in the portal vein endothelium. Similarly, co-expression of CD34 and COL1A1 can be observed in the portal vein endothelium of IPH. The portal vein endothelium of normal liver typically lacks such double-positive signals. The portal veins showing the expression of COL1A1 are irregularly distributed in an individual liver independently of the presence or absence of luminal narrowing, suggesting that luminal narrowing of the peripheral portal veins gradually progresses along with collagen deposition.

Despite evidence indicative of the involvement of
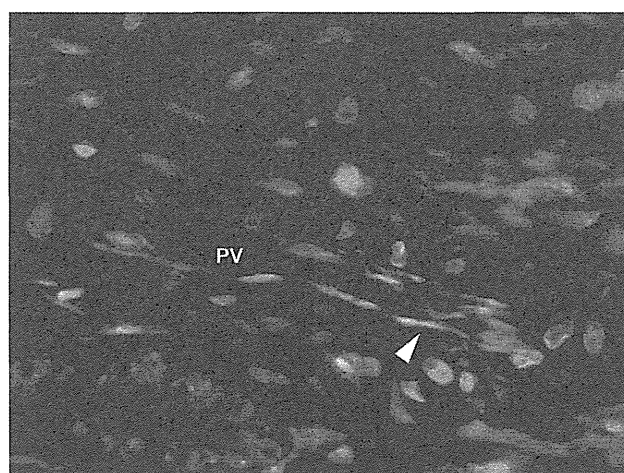
CD34/S100A4/DAPI

Fig. 5. Double immunofluorescence staining of CD34 and S100A4 protein of IPH liver. Arrowhead indicates a double-positive signal of CD34 and S100A4 in portal vein endothelium. PV, portal vein.

EndMT, the expression of S100A4 and COL1A1 is limited to only a small fraction of portal endothelial cells of IPH. Similarly, previous studies have shown that the percentage of fibroblast-specific protein-1/CD31-double-positive cells remained at 3% of total cells in a mouse model of cardiac fibrosis, although nuclear staining of pSmad2/3 was present in 30% of endothelial cells (Zeisberg et al., 2007). These results indicate that several, but not all, of the endothelial cells with positive nuclear expression of pSmad2/3 undergo phenotypic changes into myofibroblast-like cells *in vivo*, which may lead to the uneven distribution of stenotic portal tracts in IPH liver.

Co-expression of CD34 and α-SMA is rarely seen in the portal vein endothelium of IPH. These observations are consistent with the results of previous studies regarding EndMT, showing that the occurrence of colocalization of CD31 and α-SMA in the vascular endothelium was a rare event *in vivo*, compared with the

frequency of the occurrence of co-localization of CD31 and fibroblast-specific protein-1 (Zeisberg et al., 2007). Therefore, vascular endothelial cells may be able to acquire myofibroblast-like features *in vitro*, but they do not necessarily differentiate into myofibroblasts themselves *in vivo*.

Fibrogenic cytokines

The involvement of fibrogenic cytokines in the disease pathogenesis of IPH has been investigated. It has been shown that connective tissue growth factor (CTGF) is upregulated in the sera and liver tissue of IPH (Tsuneyama et al., 2002; Morikawa et al., 2007). In addition to CTGF, the serum level of TGF-ß1 in IPH patients is significantly higher than the value of healthy controls and patients with chronic viral hepatitis. TGF-ß induces CTGF in various systems. Although the cellular sources of TGF-ß1 have not been addressed, the elevated

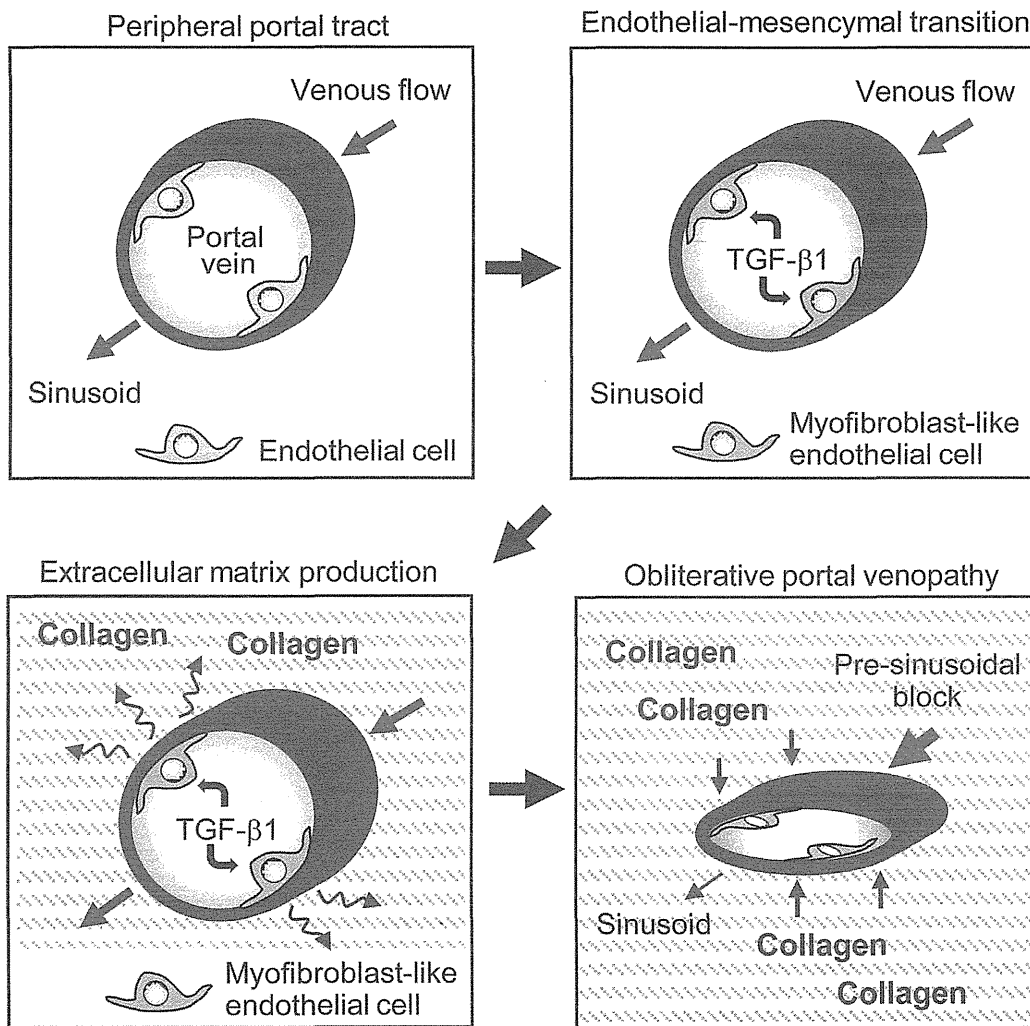Fig. 6. Proposed pathogenic mechanism of obliterative portal venopathy in IPH. TGF-ß1 induces the process of endothelial-mesenchymal transition (EndMT) in the endothelial cells of peripheral portal vein. Endothelial cells that undergo EndMT acquire the ability to express extracellular matrix molecules such as type I collagen, thereby contributing to obliterative portal venopathy and pre-sinusoidal portal hypertension.

serum TGF-ß1 level may be closely associated with the occurrence of EndMT in IPH.

The serum level of BMP-7, an antagonist of TGF-ß, is not significantly elevated in patients with IPH compared with that of healthy controls, while it is significantly elevated in patients with chronic viral hepatitis. Interestingly, there is a significant inverse correlation between the values of serum TGF-ß1 and BMP-7, suggesting the possibility that TGF-ß1 and BMP-7 have an antagonistic effect on each other's expression.

Taken together, our data suggest that EndMT plays a pivotal role in the dense collagen deposition in the portal tracts of IPHß leading to progression or even initiation of obliterative venopathy. Our proposed pathogenic mechanism of obliterative portal venopathy is illustrated in Fig. 6. From the results of our study, however, it is unclear whether the process of elastic fiber deposition in IPH liver is mediated by EndMT. Elevation of systemic TGF-ß1 level may account for the occurrence of EndMT in the absence of significant local inflammation, and BMP-7 may be a suitable therapeutic candidate for IPH.

Other endothelial dysfunction in IPH

Pathogenic mechanisms of endothelial dysfunction in IPH other than EndMT have been proposed, although the experimental data available are relatively limited because of the small amount of literature.

Immunological disorders

In relation to immunological disorders seen in IPH, the immunohistochemical expression of human leukocyte antigen D-related antigen has been demonstrated on portal microvessels (Terada et al.,

1991). Vascular cell adhesion molecule-1 (VCAM-1) is expressed in vascular endothelial cells of the IPH liver, and the serum level of soluble VCAM-1 is elevated in IPH patients (Yamaguchi et al., 1999).

Anti-endothelial cell antibodies (AECA) have been identified as circulating autoantibodies targeting the endothelial cells, and are detectable in a heterogeneous group of autoimmune and inflammatory conditions, including vasculitis (Praprotnik et al., 2001). In SSc, 20-86% of patients exhibit a positive test result for AECA (Mihai and Fervaert, 2010). IPH sera also contain AECA, which may be associated with endothelial cell damage (Sato et al., 2012). Indeed, sera containing AECA have been shown to induce the expression of pathogenic molecules such as VCAM-1 and fibrillin-1, one of the main components of microfibrils that interact with fibulin-5 during elastic fiber assembly, in cultured endothelial cells (Ahmed et al., 2006; Papa et al., 1999). Endothelial damage of the portal system is also postulated in the pathophysiology of IPH developed in patients with human immunodeficiency virus infection who have received drug treatment with didanosine (Schouten et al., 2011).

Fibroelastosis

In the peripheral portal tracts of IPH livers, immunohistochemical expression of elastin is observed in the portal vein endothelium, as well as in the portal tracts (Fig. 7, arrowheads). *In vitro*, IPH sera containing AECA induce elastin mRNA expression in HMVEC, and the amounts of elastin mRNA induced in HMVEC correlate significantly with the values of AECA of each serum used for stimulation of HMVEC (Sato et al., 2012). These results suggest a causal correlation between the induction of elastin expression in endothelial cells and the presence of AECA. Thus, AECA may induce elastin expression in endothelial cells, thereby contributing to fibroelastosis in the portal tracts of IPH.

In IPH, fibroelastosis of the major portal vein branches is also a characteristic histological feature. Fibulin-5 is an essential protein that links elastic fibers to cells and regulates fiber assembly and organization (Kielty, 2006). Fibulin-5 is preferably expressed in the vessel walls of the major portal vein branches of IPH, suggesting its role in phlebosclerosis (Sato et al., 2008). While the peripheral portal tracts of IPH totally lack the expression of fibulin-5 in spite of the presence of dense elastic fibers, the mechanism of fibroelastosis may differ between the major portal vein branches and peripheral portal tracts.

Apoptosis

It has been reported that AECA may be pathogenic by inducing endothelial cell apoptosis. Direct and dose-dependent induction of endothelial cell apoptosis by AECA from patients with SSc has been observed
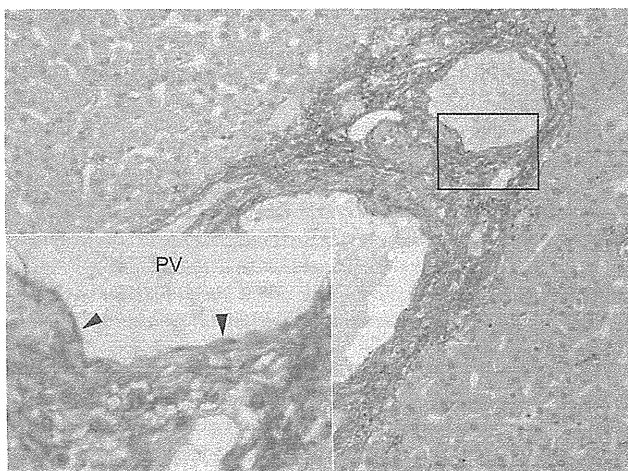

Fig. 7. Immunohistochemical expression of elastin in IPH liver. Arrowheads indicate elastin-positive portal vein endothelial cells. PV, portal vein.

(Bordron et al., 1998). In IPH, sera of patients are capable of inducing apoptosis in HMVEC (Sato et al., 2012). Apoptotic endothelial cells have been shown to secrete CTGF and promote fibrosis (Laplante et al., 2010). These observations suggest that endothelial cell apoptosis is also involved in the disease pathogenesis of IPH.

Splenomegaly

Splenomegaly of IPH is histologically characterized by proliferation of sinus endothelial cells and by irregularly widened interendothelial slits of the sinuses. Sinus lining endothelial cells of the spleen of IPH show diffuse and strong immunohistochemical expression of inducible nitric oxide synthase (iNOS) and endothelial NOS (eNOS) (Sato et al., 2007). Spleen-derived NO may affect the spleen, particularly its sinus lining cells, followed by sinus dilatation. This may in turn lead to massive splenomegaly and increased blood flow to the liver, contributing to sustained portal hypertension in IPH. Thus, the splenomegaly of IPH seems not to be simply passive congestion.

Conclusions

The pathogenic mechanisms of the development of IPH are complex, and seem to be heterogeneous. Endothelial dysfunction of the portal system may be one of the most important causative factors, and in this regard we have recently elucidated a significant role of EndMT in obliterative portal venopathy of IPH. There are limited data available from studies of the mechanism responsible for the development of IPH. To clarify the pathogenic mechanisms and to establish better treatment strategies for IPH, further extensive studies are required.

References

Ahmed S.S., Tan F.K., Arnett F.C., Jin L. and Geng Y.J. (2006). Induction of apoptosis and fibrillin 1 expression in human dermal endothelial cells by scleroderma sera containing anti-endothelial cell antibodies. Arthritis Rheum. 54, 2250-2262.

Arciniegas E., Frid M.G., Douglas I.S. and Stenmark K.R. (2007). Perspectives on endothelial-to-mesenchymal transition: potential contribution of vascular remodeling in chronic pulmonary hypertension. Am. J. Physiol. Lung Cell Mol. Physiol. 293, L1-8.

Armstrong E.J. and Bischoff J. (2004). Heart valve development: endothelial cell signaling and differentiation. Circ. Res. 95, 459-470.

Bernard P.H., Le Bail B., Cransac M., Barcina M.G., Carles J., Balabaud C. and Bioulac-Sage P. (1995). Progression from idiopathic portal hypertension to incomplete septal cirrhosis with liver failure requiring liver transplantation. J. Hepatol. 22, 495-499.

Bordron A., Dueymes M., Levy Y., Jamin C., Leroy J.P., Piette J.C., Shoenfeld Y. and Youinou P.Y. (1998). The binding of some human antiendothelial cell antibodies induces endothelial cell apoptosis. J. Clin. Invest. 101, 2029-2035.

Charles C., Clements P. and Furst D.E. (2006). Systemic sclerosis: hypothesis-driven treatment strategies. Lancet 367, 1683-1691.

Cazals-Hatem D., Hillaire S., Rudler M., Plessier A., Paradis V., Condat B., Francoz C., Denninger M.H., Durand F., Bedossa P. and Valla D.C. (2011). Obliterative portal venopathy: portal hypertension is not always present at diagnosis. J. Hepatol. 54, 455-461.

Chaudhuri V., Zhou L. and Karasek M (2007). Inflammatory cytokines induce the transformation of human dermal microvascular endothelial cells into myofibroblasts: a potential role in skin fibrogenesis. J. Cutan. Pathol. 34, 146-153

Chawla Y. and Dhiman R.K. (2008). Intrahepatic portal venopathy and related disorders of the liver. Semin. Liver Dis. 28, 270-281.

de Franchis R. (2010). Revising consensus in portal hypertension: report of the Baveno V consensus workshop on methodology of diagnosis and therapy in portal hypertension. J. Hepatol. 53, 762-768.

Eapen C.E., Nightingale P., Hubscher S.G., Lane P.J., Plant T., Velissaris D. and Elias E. (2011). Non-cirrhotic intrahepatic portal hypertension: associated gut diseases and prognostic factors. Dig. Dis. Sci. 56, 227-235.

Ghosh A.K., Nagpal V., Covington J.W., Michaels M.A. and Vaughan D.E. (2012). Molucular basis of cardiac endothelial-to-mesenchymal transition (EndMT): differential expression of microRNAs during EndMT. Cell Signal. 24, 1031-1036.

Gitler A.D., Lu M.M., Jiang Y.Q., Epstein J.A. and Gruber P.J. (2003). Molecular markers of cardiac endocardial cushion development. Dev. Dyn. 228, 643-650.

Higashiyama R., Moro T., Nakao S., Mikami K., Fukumitsu H., Ueda Y., Ikeda K., Adachi E., Bou-Gharios G., Okazaki I. and Inagaki Y. (2009). Negligible contribution of bone marrow-derived cells to collagen production during hepatic fibrogenesis in mice. Gastroenterology 137, 1459-1466.e1.

Hübscher S.G. (2011). Pathology of non-cirrhotic portal hypertension and incomplete septal cirrhosis. Diagnostic Histopathology 17, 530-538.

Isabel Fiel M., Thung S.N., Hytiroglou P., Emre S. amd Schiano T.D. (2007). Liver failure and need for liver transplantation in patients with advanced hepatoportal sclerosis. Am. J. Surg. Pathol. 31, 607-614.

Iwakiri Y. (2012). Endothelial dysfunction in the regulation of cirrhosis and portal hypertension. Liver Int. 32, 199-213.

Karasek M.A. (2007). Does transformation of microvascular endothelial cells into myofibroblasts play a key role in the etiology and pathology of fibrotic disease? Med. Hypotheses 68, 650-655.

Kielty C.M. (2006). Elastic fibers in health and disease. Expert. Rev. Mol. Med. 8, 1-23.

Kinoshita K., Iimuro Y., Otogawa K., Saila S., Inagaki Y., Nakajima Y., Kawada N., Fujimoto J., Friedman S.L. and Ikeda K. (2007). Adenovirus-mediated expression of BMP-7 suppresses the development of liver fibrosis in rats. Gut 56, 706-714.

Kitao A., Sato Y., Sawada-Kitamura S., Harada K., Sasaki M., Morikawa H., Shiomi S., Honda M., Matsui O. and Nakanuma Y. (2009). Endothelial to mesenchymal transition via transforming growth factor-beta1/Smad activation is associated with portal venous stenosis in idiopathic portal hypertension. Am. J. Pathol. 175, 616-626.

Kovacic J.C., Mercader N., Torres M., Boehm M. and Fuster V. (2012). Epithelial-to-mesenchymal and endothelial-to-mesenchymal transition: from cardiovascular development to disease. Circulation 125, 1795-1808.

Krasinskas A.M., Eghtesad B., Kamath P.S., Demetris A.J. and Abraham S.C. (2005). Liver transplantation for severe intrahepatic

noncirrhotic portal hypertension. Liver Transpl. 11, 627-634.

Laplante P., Sirois I., Raymond M.A., Kokta V., Béliveau A., Prat A., Pshezhetsky A.V. and Hébert M.J. (2010). Caspase-3-mediated secretion of connective tissue growth factor by apoptotic endothelial cells promotes fibrosis. Cell Death Differ. 17, 291-303.

Lee J.G., Ko M.K. and Kay E.P. (2012). Endothelial mesenchymal transformation mediated by IL-1,-induced FGF-2 in corneal endothelial cells. Exp. Eye Res. 95, 35-39.

Li J., Qu X., Yao J., Caruana G., Ricardo S.D., Yamamoto Y., Yamamoto H. and Bertram J.F. (2010). Blockade of endothelial-mesenchmal transition by a Smad3 inhibitor delays the early development of streptozotocin-induced diabetic nephropathy. Diabetes 59, 2612-2624.

Li Z. and Jimenez S.A. (2011). Protein kinase Cδ and c-Abl are required for transforming growth factor β induction of endothelial-mesenchymal transition *in vitro*. Arthritis Rheum. 63, 2473-2483.

Luna-Zurita L., Prados B., Grego-Bessa J., Luxán G., del Monte G., Benguría A., Adams R.H., Pérez-Pomares J.M. and de la Pompa J.L. (2010). Intergration of a Notch-dependent mesenchymal gene program and Bmp2-driven cell invasiveness regulates murine cardiac valve formation. J. Clin. Invest. 120, 3493-3507.

Mihai C. and Tervaert J.W. (2010). Anti-endothelial cell antibodies in systemic sclerosis. Ann. Rheum. Dis. 69, 319-24.

Morikawa H., Tamori A., Nishiguchi S., Enomoto M., Habu D., Kawada N. and Shiomi S. (2007). Expression of connective tissue growth factor in the human liver with idiopathic portal hypertension. Mol. Med. 13, 240-245.

Nakanuma Y., Hoso M., Sasaki M., Terada T., Katayanagi K., Nonomura A., Kurumaya H., Harada A. and Obata H. (1996). Histopathology of the liver in non-cirrhotic portal hypertension of unknown aetiology. Histopathology 28, 195-204.

Nakanuma Y., Kouda W., Nakano T., Uneno K., Tachibana S. and Araki I. (2001). A case report of early idiopathic portal hypertension. Pathol. Res. Pract. 197, 759-763.

Nakanuma Y., Tsuneyama K., Ohbu M. and Katayanagi K. (2001). Pathology and pathogenesis of idiopathic portal hypertension with an emphasis on the liver. Pathol. Res. Pract. 197, 65-76.

Nakanuma Y., Sato Y. and Kitao A. (2009). Pathology and pathogenesis of portal venopathy in idiopathic portal hypertension: hints from systemic sclerosis. Hepatol. Res. 39, 1023-1031.

Nguyen L.N., Furuya M.H., Wofraim L.A., Nguyen A.P., Houdren M.S., Campbell J.S., Knight B., Yeoh G.C., Fausto N. and Parks W.T. (2007). Transforming growth factor-beta differentially regulates oval cell and hepatocyte proliferation. Hepatology 45, 31-41.

Okudaira M., Ohbu M. and Okuda K. (2002). Idiopathic portal hypertension and its pathology. Semin. Liver Dis. 22, 59-72.

Papa N.D., Raschi E., Moroni G. Panzeri P., Borghi M.O., Ponticelli C., Tincani A., Balestrieri G. and Meroni P.L. (1999). Anti-endothelial cell IgG fractions from systemic lupus erythematosus patients bind to human endothelial cells and induce a pro-adhesive and a pro-inflammatory phenotype *in vitro*. Lupus 8, 423-429.

Piera-Velazquez S., Li Z. and Jimenez S.A. (2011). Role of endothelial-mesenchymal transition (EndoMT) in the pathogenesis of fibrotic disorders. Am. J. Pathol. 179, 1074-1080.

Popov Y. and Schuppan D. (2010). Epithelial-to-mesenchymal transition in liver fibrosis: dead or alive? Gastroenterology 139, 722-725.

Praprotnik S., Blank M., Meroni P.L., Rozman B., Eldor A. and Shoenfeld Y. (2001). Classification of anti-endothelial cell antibodies into antibodies against microvascular and macrovascular endothelial cells: the pathogenic and diagnostic implications. Arthritis Rheum. 44, 1484-1494.

Rieder F., Kessler S.P., West G.A., Bhilocha S., de la Motte C., Sadler T.M., Gopalan B., Stylianou E. and Fiocchi C. (2011). Inflammation-induced endothelial-to-mesenchymal transition: a novel mechanism of intestinal fibrosis. Am. J. Pathol. 179, 2660-2673.

Roskams T., Baptista A., Bianchi L., Burt A., Callea F., Denk H., De Groote J., Desmet V., Hubscher S., Ishak K., MacSween R., Portmann B., Poulson H., Scheuer P., Terracciano L. and Thaler H. (2003). Histopathology of portal hypertension: a practical guideline. Histopathology 42, 2-13.

Sato Y., Sawada S., Kozaka K., Harada K., Sasaki M., Matsui O. and Nakanuma Y. (2007). Significance of enhanced expression of nitric oxide syntheses in splenic sinus lining cells in altered portal hemodynamics of idiopathic portal hypertension. Dig. Dis. Sci. 52, 1987-1994.

Sato Y., Sawada S. and Nakanuma Y. (2008). Fibulin-5 is involved in phlebosclerosis of major portal vein branches associated with elastic fiber deposition in idiopathic portal hypertension. Hepatol. Res. 38, 166-173.

Sato Y., Ren X.S., Harada K., Sasaki M., Morikawa H., Shiomi S., Honda M., Kaneko S. and Nakanuma Y. (2012). Induction of elastin expression in vascular endothelial cells relates to hepatoportal sclerosis in idiopathic portal hypertension: possible link to serum anti-endothelial cell antibodies. Clin. Exp. Immunol. 167, 532-542.

Sawada S., Sato Y., Aoyama H., Harada K. and Nakanuma Y. (2007). Pathological study of idiopathic portal hypertension with an emphasis on cause of death based on records of Annuals of Pathological Autopsy Cases in Japan. J. Gastroenterol. Hepatol. 2, 204-209.

Scholten D., Reichart D., Paik Y.H., Lindert J., Bhattacharya J., Glass C.K., Brenner D.A. and Kisseleva T. (2011). Migration of fibrocytes in fobrogenic liver injury. Am. J. Pathol. 179, 189-198.

Schouten J.N., Garcia-Pagan J.C., Valla D.C. and Janssen H.L. (2011). Idiopathic noncirrhotic portal hypertension. Hepatology 54, 1071-1081.

Terada T., Nakanuma Y. and Obata H. (1991). HLA-DR expression on the microvasculature of portal tracts in idiopathic portal hypertension. Immunohistochemical characteristics and relation to portal phlebosclerosis. Arch. Pathol. Lab. Med. 115, 993-997.

Tsuneyama K., Harada K., Katayanagi K., Watanabe K., Kurumaya H., Minato H. and Nakanuma Y. (2002). Overlap of idiopathic portal hypertension and scleroderma: report of two autopsy cases and a review of literature. J. Gastroenterol. Hepatol. 17, 217-23.

Tsuneyama K., Kouda W. and Nakanuma Y. (2002). Portal and parenchymal alterations of the liver in idiopathic portal hypertension: a histological and immunohistochemical study. Pathol. Res. Pract. 198, 597-603.

Tsuneyama K., Ohba K., Zen Y., Sato Y., Niwa H., Minato H. and Nakanuma Y. (2003). A comparative histological and morphometric study of vascular changes in idiopathic portal hypertension and alcoholic fibrosis/cirrhosis. Histopathology 43, 55-61.

Wanless I.R. (1990). Micronodular transformation (nodular regenerative hyperplasia) of the liver: a report of 64 cases among 2,500 autopsies and a new classification of benign hepatocellular nodules. Hepatology 11, 787-97.

Wells R.G. (2010). The epithelial-to-mesenchymal transition in liver fibrosis: here today, gone tomorrow? Hepatology 51, 737-740.

Wynn T.A. (2008). Cellular and molecular mechanisms of fibrosis. J.

Pathol. 214, 199-210.

Yamaguchi N., Tokushige K., Haruta I., Yamauchi K. and Hayashi N. (1999). Analysis of adhesion molecules in patients with idiopathic portal hypertension. J. Gastroenterol. Hepatol. 14, 364-369.

Zeisberg E.M., Potenta S., Xie L., Zeisberg M. and Kalluri R. (2007). Discovery of endothelial to mesenchymal transition as a source for carcinoma-associated fibroblasts. Cancer Res 67, 10123-10128.

Zeisberg E.M., Tarnavski O., Zeisberg M., Dorfman A.L., McMullen J.R., Gustafsson E., Chandraker A., Yuan X., Pu W.T., Roberts A.B., Neilson E.G., Sayegh M.H., Izumo S. and Kalluri R. (2007). Endothelial-to-mesenchymal transition contributes to cardiac fibrosis. Nature Med. 13, 952-961.

Original Article

Influence of splenectomy in patients with liver cirrhosis and hypersplenism

Yoriko Nomura,[1,2,3] Masayoshi Kage,[1] Toshirou Ogata,[2] Reiichirou Kondou,[1] Hisafumi Kinoshita,[2] Kouichi Ohshima[3] and Hirohisa Yano[3]

[1]Department of Diagnostic Pathology, Kurume University Hospital, and Departments of [2]Surgery and [3]Pathology, Kurume University School of Medicine, Kurume, Japan

Aim: Splenectomy improves hypersplenic thrombocytopenia in cirrhotic patients with hypersplenism. However, the long-term influence of splenectomy has not been clarified. We examined whether splenectomy improved liver fibrosis and caused immunological changes.

Methods: We collected liver and spleen specimens and peripheral blood (PB) from 26 patients with hepatitis C virus-related liver cirrhosis. An immunohistochemical examination of CD4, CD8, forkhead box P3, granzyme B and transforming growth factor-β1, and Masson-trichrome stain were performed in spleen and liver tissues and in seven cases of follow-up liver biopsy sections obtained after splenectomy. We obtained PB before and at various intervals after splenectomy. We also examined the ratio of CD4$^+$ and CD8$^+$ lymphocytes in PB using flow cytometry.

Results: We observed improvements in liver fibrosis in four biopsy specimens obtained after splenectomy, in which

fibrotic areas significantly decreased from 19.5% to 8.2% ($P < 0.05$). Increases were also observed in the ratio of CD8$^+$ cells in PB after splenectomy, which resulted in a significant decrease in the CD4$^+$/CD8$^+$ ratio ($P < 0.001$). The carcinogenic rate in patients with a CD4$^+$: CD8$^+$ ratio that decreased by more than 0.5 at 1 month after splenectomy was significantly lower than that in patients with a ratio that decreased by less than 0.5 ($P < 0.05$).

Conclusion: Splenectomy may improve liver fibrosis and cause beneficial immunological changes in cirrhotic patients with hepatitis. Improvements in antitumor mechanisms can be also expected.

Key words: CD4$^+$ cytotoxic T lymphocytes, CD8$^+$ cytotoxic T lymphocytes, liver cirrhosis, liver fibrosis, splenectomy

INTRODUCTION

SPLENECTOMY IS A common treatment used to improve hypersplenic thrombocytopenia in cirrhotic patients with splenomegaly in Japan.[1–7] Splenectomy has recently been applied as another option to cure hepatocellular carcinoma (HCC) and for cirrhotic patients with no potential donor for liver transplantation. Thus, the clinical application of splenectomy has been expanded; however, the immunophysiology of the spleen in cirrhotic patients and the long-term outcome after splenectomy have not been clarified.[8–14] This study was designed to clarify the long-term changes and prediction of HCC development following splenectomy,

with a focus on hepatic fibrosis and immunology. Regarding hepatic fibrosis, Akahoshi *et al.* reported that transforming growth factor (TGF)-β1 derived from the spleen could have an inhibitory role in healing liver cirrhosis by inhibiting the regeneration of the damaged liver[15] and we experimentally confirmed that splenectomy significantly reduced liver fibrosis and decreased TGF-β1 in the serum of a dimethylnitrosamine-induced cirrhotic rat model.[16] However, no studies have yet described a reduction in hepatic fibrosis following splenectomy in humans.

The spleen plays an important role in the immune response; however, the functional aspects of the spleen in cirrhotic patients with hepatitis C virus (HCV) infection are largely unknown.[2,17] Hashimoto *et al.* reported that splenectomy was followed by an increased ratio of interferon (IFN)-γ to interleukin (IL)-10 and a reduction in programmed death (PD)-1-expressing CD4$^+$ T cells in peripheral blood (PB).[7] In order to clarify chronological changes in immunity after splenectomy, we examined liver and spleen tissues and sera to assess CD4$^+$ and

1

CD8^{+} cytotoxic T lymphocytes (CTL) and regulatory T (Treg) cells.[18,19] TGF-β1 was also examined as it is a multifunctional cytokine that inhibits the growth of tumor cells[20-23] and liver regeneration by facilitating tissue fibrosis in the liver.[16]

Host immunoreactions against cancer were shown to be closely related to cellular immunity by CD8^{+} CTL and Treg cells, produced by T lymphocytes, and CD8^{+} CTL in particular.[19] The level of Treg cells, characterized by the expression of forkhead box P3 (FOXP3) transcription factor in the PB and tumor tissues of patients with HCC, was elevated and appeared to be negatively correlated with prognosis.[21,24,25]

In the present study, we examined whether splenectomy could improve liver fibrosis, cause immunological changes, especially in CTL, or be used to predict the risk of carcinogenesis.

METHODS

Patients and samples (Table 1)

AT THE DEPARTMENT of Surgery, Kurume University Hospital, 26 patients (Child A, 16 cases; Child B/C, 10 cases) with HCV-related liver cirrhosis (with HCC, seven cases; without HCC, 19 cases) and hypersplenism underwent splenectomy (splenectomy group). The purpose of splenectomy was to improve hypersplenic thrombocytopenia and introduce IFN for clearance of the HCV virus. Forty-eight patients who underwent hepatectomy due to liver tumors were recruited as controls (control group 1). PB samples from 10 healthy adult volunteers (control group 2) and spleen tissues obtained by splenectomy from seven patients because of trauma (control group 3) were also used as controls. In addition, all patients were HIV negative. Patients received no medical treatment except splenectomy during the study period. All samples were studied after obtaining the appropriate institutional informed consent. We also obtained permission from the ethical review board.

Liver tissue

A total of 26 pieces from the resected liver specimens of patients with HCV-related liver cirrhosis and hypersplenism who underwent splenectomy were also examined for the immunohistochemical expression of CD4^{+}

Table 1 Subject characteristics

Variables	Results
Splenectomy group: splenectomy (26 cases, seven with HCC, 19 without HCC)	
Age, median (range)	60.4 ± 1.36 (46–75)
Sex (male/female)	12/14
Virus infection (HCV[+])	26
Fibrosis (F0/F1/F2/F3/F4)	0/0/0/0/26
Child–Pugh classification (A/B/C)	16/8/2
Tumor nodules (presence/absence)	7/19
Weight of the spleen (g)	510.4 ± 55.6 (125–1065)
Control 1: hepatectomy with HCC (48 cases)	
Age, median (range)	70.5 ± 1.33 (42–82)
Sex, male/female	29/19
Virus infection (HCV[+])	40
Fibrosis (F0/F1/F2/F3/F4)	8/10/10/10/10
Tumor nodules (presence/absence)	48/0
Control 2: healthy adult volunteers (10 cases)	
Age, median (range)	40.1 ± 2.97 (32–57)
Sex (male/female)	3/7
Control 3: splenectomy control (seven cases; trauma)	
Age, median (range)	59.8 ± 6.27 (36–82)
Sex (male/female)	6/1

Continuous variables are expressed as the mean ± standard deviation.
Fibrosis: F0, no fibrosis in the portal tract; F1, portal fibrosis without septa; F2, portal fibrosis with few septa; F3, numerous septa without cirrhosis; F4, cirrhosis.
HCC, hepatocellular carcinoma; HCV, hepatitis C virus.

Spleen

FOXP3   CD4   CD8   Granzyme B   TGF-β1
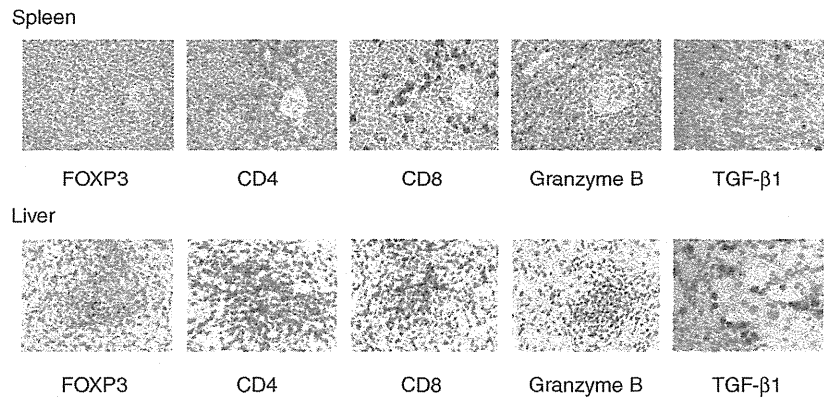
Liver

Figure 1 Immunohistochemical staining of spleen and liver specimens with forkhead box P3 (FOXP3), CD4, CD8, granzyme B and transforming growth factor (TGF)-β1 in the spleen and liver.

FOXP3   CD4   CD8   Granzyme B   TGF-β1

lymphocytes, CD8⁺ lymphocytes, FOXP3, granzyme B and TGF-β1 positive cells (Fig. 1). We classified liver specimens into five stages according to the degree of fibrosis as follows: F0, no fibrosis in the portal tract; F1, portal fibrosis without septa; F2, portal fibrosis with a few septa; F3, numerous septa without cirrhosis; and F4, cirrhosis. We collected resected liver specimens from 10 cases each of F1, F2, F3 and F4 with HCV-related liver disease. We also collected specimens from eight cases of liver hemangioma of F0 with both negative hepatitis B surface antigen and HCV antibody. Follow-up liver biopsy sections were obtained from the same part of the liver if possible from seven of the 26 patients at various intervals after splenectomy (Table 2). These sections were used for CD4 and CD8 immunostaining and Masson-trichrome staining for the morphometric evaluation of fibrotic areas.

Spleen tissue

A total of 26 spleens with HCV-related liver cirrhosis and hypersplenism were examined for the immunohis-

tochemical expression of CD4 positive lymphocytes, CD8 positive lymphocytes, FOXP3, granzyme B and TGF-β1 positive cells. We measured the same parameters in spleens from the seven control cases in control group 3 as a non-cirrhotic control (Fig. 1). Spleen and liver tissues were pathologically assessed by two pathologists (Y. N. and M. K.).

Peripheral blood cells

Peripheral blood samples were serially collected from 26 patients with HCV-related liver cirrhosis and hypersplenism just before and 14 days, 1 month, 3 months, 6 months and 1 year after splenectomy. We examined the ratio of CD4⁺ T cells to all lymphocytes, CD8⁺ T cells to all lymphocytes, and the CD4⁺/CD8⁺ ratio in PB samples using flow cytometry. TGF-β1 levels in PB were also measured using enzyme-linked immunoassays in the sera just before and 14 days, 1 month, 3 months, 6 months and 1 year after splenectomy. Patients were excluded from the protocol if IFN or other therapeutics were introduced for the liver disease. Ten healthy adult

Table 2 Clinical and pathological findings of 7 patients who underwent follow-up liver biopsies

Case	Age	Sex	Activity	Child–Pugh (score)	CD4/8	Follow-up range (days)	Before (%)	After (%)	Rate of change
1	63	M	1	A (5)	1.73	581	6.59	18.31	2.78
2	58	M	2	A (5)	1.22	24	7.38	8.99	1.22
3	58	M	2	B (7)	1.57	333	9.92	12.02	1.21
4	52	M	2	A (5)	1.08	431	16.71	5.10	0.30
5	74	M	2	A (6)	0.63	353	20.02	6.31	0.32
6	53	F	2	A (6)	0.93	248	30.03	13.34	0.44
7	59	M	2	A (5)	0.95	42	11.27	8.05	0.71

Activity: A0, none; A1, portal inflammation only; A2, mild interface hepatitis; A3, moderate interface hepatitis; A4, severe interface hepatitis.
Before, the rate of fibrotic areas before splenectomy; after, the rate of fibrotic areas after splenectomy.

volunteers in control group 2 without a history of liver disease or splenomegaly were also recruited as controls, and samples were collected only once.

Immunohistochemical analysis

All fresh specimens were fixed by 10% formalin, and paraffin-embedded tissue samples were cut at a thickness of 4 μm, examined on a coated slide glass, and labeled with the following antibodies using the Bond-Max autostainer (Leica Microsystems, Newcastle, UK) and DAKO autostainer (DakoCytomation, Glostrup, Denmark): CD4 (×200; Leica Microsystems), CD8 (×200; Leica Microsystems), granzyme B (×50; Leica Microsystems), TGF-β1 (×300; Santa Cruz Biotechnology, Heidelberg, Germany) and FOXP3 (×600; Abcam, Cambridge, MA, USA).

Immunohistochemical examinations with CD4, CD8, granzyme B and TGF-β1 were performed on the same fully automated Bond-Max system using onboard heat-induced antigen retrieval with ER2 for 10 min and the Refine polymer detection system (Leica Microsystems). 3,3'-Diaminobenzidine-tetrachloride (DAB) was used as the chromogen for all immunostaining. FOXP3 immunostaining was carried out using the DAKO autostainer with the ChemMate ENVISION method (DakoCytomation). Briefly, specimens were boiled in a microwave for 30 min in 1 mmol/L ethylenediamine-tetraacetic acid, pH 9.0, and target retrieval solution (DakoCytomation) to recover antigens, and the specimens were then incubated with the antibody at 4°C overnight. After washing in Tris-buffered saline (TBS), slides were incubated with the labeled polymer-horseradish peroxidase secondary antibody for 30 min at room temperature. After washing in TBS, slides were visualized using DAB.

Detection of immune function using flow cytometry

T-lymphocyte subsets in PB such as CD4, CD8 and CD4/8 were determined by flow cytometry, and the monoclonal antibodies of CD4 and CD8 (labeled CD4-FITC, CD-8-RD1) were purchased from Beckman Coulter (Danvers, MA, USA).

Result assessment

For assessment criteria for lymphocytes and other positive cell counts, the number of lymphocytes and other positive cells were counted in 20 areas within a specimen under high-power fields (×40 objective, ×10 eyepiece). Ten areas of white and red pulp were assessed in

the spleen, and 10 periportal areas and 10 hepatic lobule areas (Fig. 1) were assessed in a non-tumor area of the liver.

Morphometric analysis (computer image analysis) was performed in the following manner on specimens stained with Masson-trichrome. The equipment used to assess morphometry consisted of a light microscope, a three-color charge-coupled device camera, and a high resolution computer image analysis system (WinRooF software package version 6.1; Mitani, Fukui, Japan). The magnified images (×40) of specimens captured by the camera mounted on the microscope were sent to the image analyzing computer. Collagen fibers stained with Masson-trichrome were then selected. In this study, this scanning procedure was repeated 10 times in random areas. The area of fibrosis (AF) was defined as the ratio (%) of the whole area of collagen fibers to that of the liver tissue scanned.

Statistical analyses

Statistical analysis was performed using Student's *t*-test. A *P*-value of less than 0.05 was considered to be significant.

The follow-up time was calculated as the interval between the date of surgery and intervention of the medical treatment, last follow up or recognition of HCC. Survival rates or failure rates were analyzed with the Kaplan–Meier method using the log–rank test to assess differences between curves. A *P*-value of less than 0.05 was considered to be significant. Statistical calculations were performed using the JMP software package (release 10, SAS Institute, Cary, NC, USA).

RESULTS

Liver

IN THE SEVEN follow-up liver biopsy sections (Table 2) available for histological examination, liver fibrosis in the hepatic lobules improved from F4 to F3 in four cases (cases 4–7: average, 268.5 ± 168.6 days; range, 42–431 days) (Fig. 2a). Improvements were not observed in the remaining three cases (cases 1–3: average, 312 ± 279.1 days; range, 24–581 days) (Fig. 2b). There were no statistical differences in the duration between the improvement cases and non-improvement cases (*P* = 0.80). Conducting an evaluation was difficult because only a few specimens were available; however, no significant differences in clinical profiles were observed among the seven patients. In four of these cases (cases 4–7), the ratio significantly

(a)

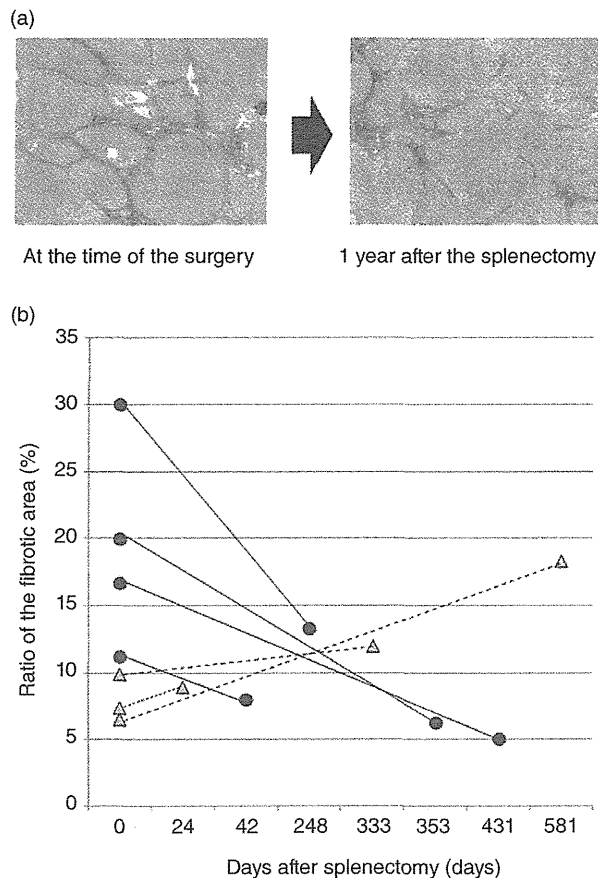At the time of the surgery   1 year after the splenectomy

(b)

Figure 2 (a) Improvements in liver fibrosis. Distortions in hepatic lobules improved in the liver biopsy sections of four cases after splenectomy, and fibrotic areas significantly decreased from 19.5% to 8.2% in these sections. (b) Changes in the fibrotic areas of seven patients at various intervals. ●—● shows patients in whom the fibrotic area significantly decreased after splenectomy. ▲⋯▲ shows patients in whom fibrosis deteriorated.

decreased from 19.5% to 8.2% ($P < 0.05$) (Fig. 2b), while the average AF in the remaining three cases (cases 1–3) increased from 8.0% to 13.1% ($P = 0.15$). The four cases of improved fibrosis were all Child–Pugh A, and one of the three cases that showed no improvement was Child–Pugh B. In addition, AF before splenectomy was slightly higher in the improvement cases than in the non-improvement cases, while the CD4+/CD8+ ratio before splenectomy was lower in the improvement cases than in the non-improvement cases ($P < 0.05$). Histopathologically, CD4+ and CD8+ lymphocytes were mainly seen in the periportal area, and CD4+ lympho-

cytes were rarely seen in the hepatic lobules. The epithelial cells, fibroblasts, monocytes and macrophages also produced TGF-β1.[4,21,26] However, we picked up and counted the TGF-β1 positive cells that were seen in the lymphocytes and found that these cells were distributed diffusely in the hepatic lobules and periportal area. The distribution pattern of Treg and granzyme B was the same as that of CD4+ and CD8+ lymphocytes, respectively. No significant differences were observed in the CD4+/CD8+ ratio ($P = 0.21$) in liver specimens, regardless of the association of HCC. The CD4+/CD8+ ratio ($P < 0.05$) and FOXP3/CD4+ ratio ($P < 0.001$) significantly increased with the progression of liver fibrosis (from F0 to F4). However, the granzyme B/CD8+ ratio was approximately constant, and was unrelated to the progression of liver fibrosis ($P = 0.32$).

The number of TGF-β1 positive cells in livers with HCC was slightly higher than that in livers without ($P = 0.06$), and the number of TGF-β1 positive cells also significantly increased with the progression of liver fibrosis ($P < 0.001$) (Fig. 3).

Spleen

Histopathologically, CD4+ and CD8+ lymphocytes were found more in the white pulp than in the red pulp. The results of the clinicopathological analysis showed that the CD4+/CD8+ ratio in spleens with HCV-related liver cirrhosis and hypersplenism was higher than that in the spleens of control group 3 ($P = 0.06$). The FOXP3/CD4+ ratio in control group 3 was higher than that in cases of hypersplenism ($P < 0.05$), and no significant differences
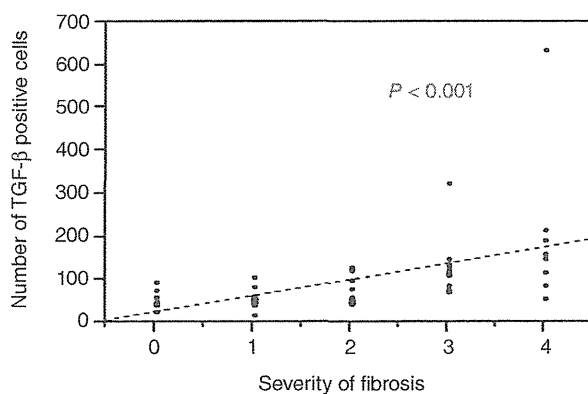
Figure 3 Correlation between transforming growth factor (TGF)-β1 positive cells and fibrosis in the liver. The number of TGF-β1 positive cells also significantly increased with the progression of liver fibrosis.
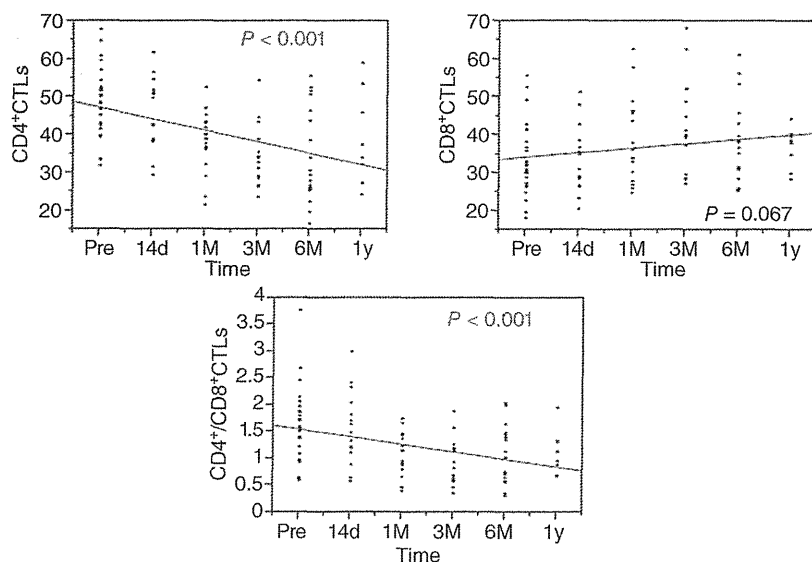
Figure 4 Changes in peripheral blood after splenectomy. pre, preoperative; d, days; M, months; y, year. The ratio of CD4^{+} T cells to all lymphocytes significantly decreased 1 year after splenectomy, while the ratio of CD8^{+} T cells to all lymphocytes slightly increased, resulting in a significant decrease in the CD4^{+}/CD8^{+} ratio.

in the granzyme B/CD8^{+} ratio ($P = 0.82$) were observed between the splenectomy group and control group 3 (data not shown).

Peripheral blood

The ratio of CD4^{+} T cells to all lymphocytes and the CD4^{+}/CD8^{+} ratio in PB samples obtained from 26 patients before splenectomy were significantly higher than those from control group 2 ($P < 0.01$, $P < 0.05$). In contrast, the ratio of CD4^{+} T cells to all lymphocytes significantly decreased 1 year after splenectomy ($P < 0.001$), while the ratio of CD8^{+} T cells to all lymphocytes slightly increased ($P = 0.07$), resulting in a significant decrease in the CD4^{+}/CD8^{+} ratio ($P < 0.001$) (Fig. 4).

Transforming growth factor-β levels were higher in PB samples from patients with HCC than in those without. TGF-β1 levels slightly increased in PB samples 1 month after splenectomy, then decreased, and subsequently returned to the level measured before splenectomy in 1 year.

Relationship of the CD4^{+}/CD8^{+} ratio between PB and the spleen or liver

In the splenectomy group, the CD4^{+}/CD8^{+} ratio in PB had a significant positive correlation with the CD4^{+}/CD8^{+} ratio in the spleen ($P < 0.05$), and was also positively associated with the liver ($P = 0.07$). As a result, a

significant positive correlation was observed between the CD4^{+}/CD8^{+} ratio in the spleen and that in the liver ($P < 0.05$) (Fig. 5).

Correlation between the CD4^{+}/CD8^{+} ratio and clinical prognosis

We compared the CD4^{+}/CD8^{+} ratio between PB obtained pre-splenectomy and 1 month after splenectomy ($n = 19$). The median of differences between pre-splenectomy and 1 month after splenectomy was 0.5. The occurrence of HCC was significantly lower in cases in which the difference in the CD4^{+}/CD8^{+} ratio between the perioperative period and 1 month later was over 0.5 (≥ 0.5 vs < 0.5, $P < 0.05$) (Fig. 6a).

A positive correlation in PB was observed between the CD4^{+}/CD8^{+} ratio before splenectomy and differences in the CD4^{+}/CD8^{+} ratio between pre-splenectomy and 1 month after splenectomy ($P < 0.001$). As the median of the preoperative CD4^{+}/CD8^{+} ratio was 1.7, the postoperative (1 month after splenectomy) CD4^{+}/CD8^{+} ratio significantly decreased in groups in which the preoperative value was larger than 1.7 (Fig. 6b,c).

DISCUSSION

PREVIOUS STUDIES HAVE shown that splenectomy was effective in improving pancytopenia, the decompression of portal hyperpressure and liver function.[1,2,27,28] Morinaga *et al.* reported that splenectomy
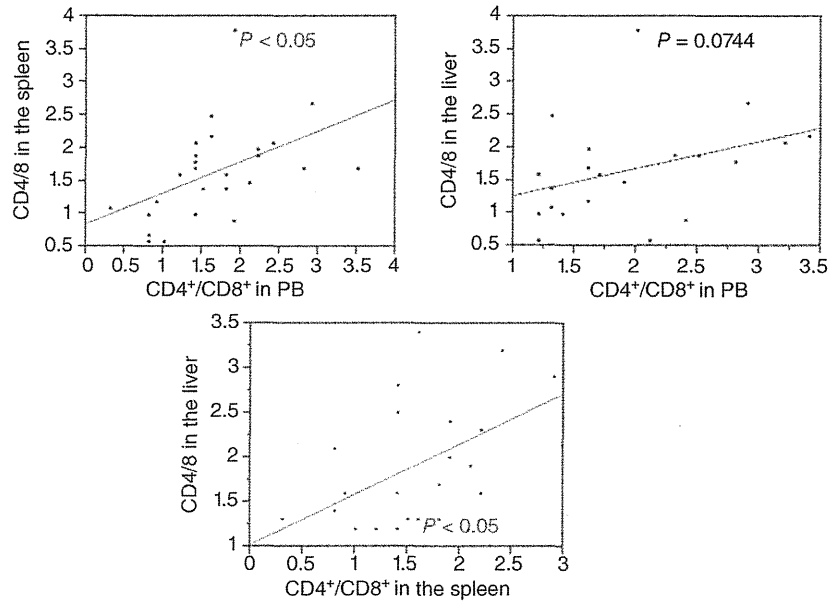
Figure 5 Correlations between the CD4+/CD8+ ratios in the spleen, liver and peripheral blood (PB). A significant positive correlation was observed between the CD4+/CD8+ ratio in the spleen and that in the liver.

significantly improved liver fibrosis with a reduction in plasma TGF-β1 levels in the rat. However, all these reports of hepatic fibrosis were conducted in animal models[1,16,29,30] whereas the present study described improvements in liver fibrosis after splenectomy in humans. Interestingly, the CD4+/CD8+ ratio changed after splenectomy without other treatment. However, many confounding factors may be implicated in this change. It is likely that patients with a high fibrotic area in their liver specimens had a high CD4+/CD8+ ratio;

Figure 6 (a) Correlation between carcinogenesis, the perioperative period and 1 month later. The occurrence of hepatocellular carcinoma was significantly lower in cases in which the difference in the CD4+/CD8+ ratio between the perioperative period and 1 month later was over 0.5. (b,c) Correlation in peripheral blood (PB) between the CD4+/CD8+ ratio before surgery and differences in the CD4+/CD8+ ratios before splenectomy and 1 month after splenectomy. (b) A positive correlation in PB was observed between the CD4+/CD8+ ratio before splenectomy and differences in the CD4+/CD8+ ratio between pre-splenectomy and 1 month after splenectomy. (c) The postoperative (1 month after splenectomy) CD4+/CD8+ ratio significantly decreased in groups in which the preoperative value was larger than 1.7. ■, pre; ▩, post.